THE ASTROPHYSICAL JOURNAL, 257:204–213, 1982 June 1

IUE OBSERVATIONS OF THE PECULIAR STAR RX PUPPIS

MINAS KAFATOS[1]
Department of Physics, George Mason University

AND

A. G. MICHALITSIANOS AND W. A. FEIBELMAN
Laboratory for Astronomy and Solar Physics, NASA Goddard Space Flight Center
Received 1981 June 12; accepted 1981 December 11

ABSTRACT

We have obtained the first high-dispersion observations of RX Pup in the wavelength region 1200–2000 Å with the *International Ultraviolet Explorer*. RX Pup has been classified a symbiotic star and has been compared to slow novae as well as to η Carinae. The anomalies that we observed in high-excitation lines in RX Pup such as He II, O III], C III], C IV, and Si III] that show split line profiles, Doppler displaced multiple components, and possible inverse P Cygni profiles in N III] and N IV] suggest dynamic activity in circumstellar material that probably has the form of rings and/or gas streamers between the cool giant and the hot companion. The continuum observed by us in low dispersion is fairly flat in the wavelength region 1200–2000 Å and rises toward longer wavelengths in the region 2000–3200 Å. It cannot be due to a star earlier than A0 II. Alternatively it may be from an accretion disk. We find electron densities in the line-emitting region in the range 10^9–10^{11} cm^{-3}, temperatures in the range 10,000–20,000 K, and linear sizes $\lesssim$ a few $\times 10^{13}$ cm. We find that the photoionizing radiation may be due to the presence of an unseen, hot subdwarf with most probable effective temperature in the range 75,000–90,000 K. Alternatively it may be due to an accretion disk around a secondary with boundary layer temperature $\sim 10^5$ K. Short-range as well as long-range monitoring of this very interesting object in the far-UV would be very helpful in understanding the nature of its peculiar properties and the connection between slow novae and symbiotic stars.

Subject headings: stars: binaries — stars: combination spectra — stars: individual — ultraviolet: spectra

I. INTRODUCTION

When observed by Swings and Struve (1941), the peculiar emission-line object RX Puppis displayed a rich high-excitation emission spectrum featuring intense He II, [Fe VII], [Ne V], and other lines of >100 eV ionization potential. As noted by Swings (1970), no evidence of a late-type absorption spectrum was ever found, even though its emission spectrum resembled that typically observed in symbiotic stars. It is classified as a symbiotic variable in the *General Catalogue of Variable Stars*.

Observations by Sanduleak and Stephenson (1973) revealed low-excitation emission lines. An M star could not be confirmed in slit spectra taken by Swings and Klutz (1976) and Klutz, Simonetto, and Swings (1978). Swings and Klutz (1976) suggested, on the basis of decreased emission excitation in RX Pup between 1941 and 1968, and by the existence of an infrared excess (Swings and Allen 1972), that RX Pup could be compared to η Carinae or slow-nova–like objects. Feast, Robertson, and Catchpole (1977) detected variability in the 1–4 μm region and argued that this variability could be explained by the presence of a Mira variable. Subsequently, Klutz, Simonetto, and Swings (1978) discounted the presence of an M star in the system. On the basis of the existence of absorption lines of Fe II, He I, O I, and Mg II and the colors they argued that the continuum of RX Pup is that of a late B or early A giant ($M_v \sim -3$). They, moreover, attribute the variability to variations of a circumstellar dust shell around the B giant.

The presence of H_2O and CO absorption in RX Pup was recently demonstrated by means of 2 μm spectroscopy (Barton, Phillips, and Allen 1979). On the basis of the stream absorption band at 1.9 μm they confirmed the existence of a Mira variable ($T_{\rm eff} \sim 2400$ K). They conclude that RX Pup is a symbiotic binary star in which the primary is a Mira variable. Recently, Whitelock (1981) has reported a 580^d period for the Mira in RX Pup. Night to night variations in the Balmer line intensities in 1975 March were reported by Swings and Klutz (1976). Multicomponent P Cygni profiles of the Balmer lines and the stronger Fe II lines were detected in 1976 (Klutz, Simonetto, and Swings 1978), and sharp blueshifted absorptions in the Balmer lines ranging from -1100 to -230 km s^{-1} were seen in 1975, 1976, and 1977. Moreover, the 1977 Hγ or Hδ profiles show a strong emission line with a very steep blue wing, a sharp

[1] Work supported by NASA grant NSG 5371.

emission peak, and a broad red wing with absorption at +250 km s^{-1} (Klutz, Simonetto, and Swings 1978).

We present here the first set of high-dispersion UV observations of RX Pup. Anomalous line profile structure observed in a number of high-excitation emission lines is discussed in context with a model that includes streams and complex mass motions in the system.

II. OBSERVATIONS AND DATA ANALYSIS

a) UV Lines and Continuum

IUE spectral data were obtained exclusively in the large 10″ × 20″ entrance aperture of the satellite spectrometer (Boggess *et al.* 1978). The Fine Error Sensor (FES) monitor on *IUE* obtained an apparent magnitude $m_v \approx 10$.

We obtained *IUE* low-resolution short wavelength prime (SWP) and long wavelength redundant (LWR) spectra of RX Puppis on 1980 September 20 as well as one 102 min high-dispersion SWP spectrum, all under *IUE* observing program ZACAM. We find split line profiles of the He II 1640.3 Å, O III] 1660.8 and 1666.1 Å, and Si III] 1892 Å lines; multiple emission components in the C IV 1548.2 and 1550.8 Å lines; and asymmetric profiles in the Si IV 1393.7, N IV] 1486.5 Å, and N III] 1749.7 Å, 1754 Å lines. The low-resolution spectra reveal lines in order of increasing wavelength of O I, Si IV, O IV], N IV], C IV, He II, O III], N III], Si II, Si III], C III] in the LWR and C II] + [O III], He II, Mg II, [Ar IV] + He I and a number of O III lines.

Table 1 presents the line identifications in the high-

TABLE 1

LINE IDENTIFICATION AND ABSOLUTE FLUX

Ionic Transition	Wavelength (Å)[a]	Wavelength of *IUE* Feature (Å)	Flux[b] (ergs cm^{-2} s^{-1})	Comments[c]
C III	1174.933 + 1175.263	1174.70	...	
C III	1175.590 + 1175.711 + 1175.987	1175.53	...	
C III	1176.37	1176.66	...	
C I?	1302.169	1302.47		
O I	1304.518	1304.86	7.0×10^{-13}	
O I	1306.029	1306.27		
Si IV	1393.755	1393.86, 1394.14		emission components (e)
		1394.64		possibly absorption (a)
O IV]	1397.20	1396.83		
O IV]	1399.774	1399.92	1.83×10^{-12}	
O IV]	1401.156	1400.55, 1400.88		(e)
O IV]	1404.812	1404.08, 1404.32, 1404.49		(e)
O IV]	1407.386	1407.42		
N IV]	1486.496	1486.59	1.97×10^{-12}	(e)
		1487.54		(a)?
C IV	1548.185	1548.24, 1548.42, 1548.78	1.05×10^{-11}	(e)
C IV	1550.774	1550.74, 1550.94, 1551.18		(e)
[Ne V]?	1575.2	1574.9	...	
He II	1640.332	1640.48, 1641.24	3.57×10^{-12}	(e)
O III]	1660.803	1660.65, 1660.91	5.1×10^{-12}	(e)
O III]	1666.153	1665.95, 1666.31		(e)
N III]	1749.674	1749.73		(e)
		1750.58	3.26×10^{-12}	(a)?
N III]	1753.986	1753.89		(e)
		1754.50		(a)?
[Ne III]?	1814.8	1814.86	...	
Si II	1808.012	1808.26	4.46×10^{-13}	
Si II	1816.928 + 1817.451	1817.05		
Si III]	1892.030	1891.86, 1892.25	3.16×10^{-12}	(e)
C III]	1908.734	1908.72	6.94×10^{-12}	
C II] + [O III]?	2325.4 + 2326.93 + 2328.12 + 2321.1	2330.4	5.53×10^{-13}	
He II	2511.2	2511.8	1.19×10^{-12}	
He II	2733.3	2735.4	8.83×10^{-13}	
Mg II	2795.5 + 2802.7	2799.4	2.32×10^{-12}	
He I + [Ar IV]?	2829.08 + 2853.6	2843.6	3.01×10^{-12}	
He I + O III	3013.7 + 3024.57	3025.2	5.26×10^{-13}	
O III	3047.13	3047.6	1.74×10^{-12}	
O III	3132.86	3135.2	6.46×10^{-12}	
He I	3187.75	3191.6	1.06×10^{-12}	

[a] All short wavelengths are from Kelly and Palumbo 1973; forbidden line wavelengths are from Wiese, Smith, and Glennon 1966; all long wavelengths (>2000 Å) are from Kelly 1979).

[b] Absolute fluxes are obtained from low dispersion spectra (~6 Å respectral resolution).

[c] Multiple emission components are indicated by (e). Si IV, N IV], and N III] indicate possible absorption redward of the rest wavelength, (a); these lines have an extended emission blue wing, (e). All other features are emission lines.

dispersion (0.1 Å resolution) SWP spectrum and the line identifications in the low-dispersion (6 Å resolution) LWR spectrum. In the last column we present the line fluxes of the most prominent features, where fluxes are obtained from low-dispersion spectra only. The *IUE* data tapes were analyzed using the data reduction routines developed in FORTH at NASA Goddard Space Flight Center on the PDP-11/40 interactive computer system (Fahey and Klinglesmith 1979).

As can be seen from Table 1, there is considerable structure in the lines observed. The emission components are indicated by (e) in the fifth column, while possible absorption is indicated by (a). The C IV doublet shows components at the rest wavelengths of the two lines as well as two components redshifted from the rest wavelengths by ~ 40 km s^{-1} and ~ 90 km s^{-1}. We note that the internal errors of *IUE* of ~ 0.05–0.10 Å (Bruhweiler, Kondo, and McCluskey 1980) correspond to ~ 10–20 km s^{-1} uncertainty at the C IV wavelengths. The He II 1640.33 Å line shows two components, the strongest centered near the rest wavelength, the weaker redshifted by ~ 170 km s^{-1}. The O III] 1660.80 Å and 1666.15 Å lines show two components, each located more or less symmetrically shortward and longward of the rest wavelength. The two components have a total separation of ~ 55 km s^{-1}, indicating possibly the presence of a ring system. The Si III] 1892.03 Å line shows a similar structure with a total separation of the two components ~ 60 km s^{-1}. Due to the uncertainties involved, the O III] and Si III] lines could arise from identical regions. The C III] 1908.7 Å line shows a single component. Finally, the N IV] and N III] lines show asymmetric profiles. We see emission components in which the blue wings of the lines are extended with emission in the red wing dropping abruptly. The situation may be similar in the Si IV line, although in this case the high-dispersion signal is weak and, therefore, the structure uncertain. We note that the extended shortward wing emission observed in a number of the spectral lines observed in the UV are exactly opposite to what Klutz, Simonetto, and Swings (1978) observed in the profiles of Hγ, Hδ in 1977. It is obvious that such complex line structure should be monitored for time variations. Because the profiles change dramatically as one proceeds through different stages of ionization, one should not be surprised to see large changes in emission as the geometry of the object alters. The separation of the N IV] peak from the sharply dropping longward wing of this line is ~ 200 km s^{-1} and ~ 150 km s^{-1} for the N III] lines.

From the above discussion, we see that there is a tendency for larger velocity separations to be associated with higher ionization stages, the largest ones seen in the He II, N IV] profiles. Moreover, it is hard to see how a single object could account for such complicated profiles. It should be pointed out, however, that no systematic radial velocity change has so far been detected. The predominance of longward emission—or absorption—features probably argues for a gas stream from the red component falling toward a hot secondary. Symmetric components—as seen in the O III], Si III] lines—argue for a ring system. Rotation as an explanation of doubling of optical emission lines has also been proposed by Allen for a number of symbiotics (see Allen 1980). We suspect that the multiple component structure of the lines in RX Pup would change with time as the two stars and the gas in between them change their orientation with respect to the Earth, and this would be an easy test for binarity. In this picture, higher orbital velocities would be associated with higher ionization closer to the hot secondary.

Finally, we note that the 1548 Å component of C IV is weaker than the 1550 Å component, although the expected ratio should be 2:1 for an optically thin gas and 1:1 for an optically thick one. A similar situation prevails in other symbiotic stars, such as AG Peg (Keyes and Plavec 1980), Z And (Altamore *et al.* 1981), and V1016 Cyg (Nussbaumer and Schild 1981). Other resonance lines—N V, Si IV—show this effect too. Collisional de-excitation of the upper level and high optical depths may contribute to an alteration of the 2:1 ratio, although Nussbaumer and Schild (1981) have shown that this meets with certain difficulties and may not be necessary to involve such mechanisms: a hot ($T \sim 10^5$ K) diffuse interstellar medium may be sufficient. Since the presence of this component of the interstellar medium has recently been detected with *IUE* near the Sun (Bruhweiler and Kondo 1981), this mechanism is very plausible. It is still difficult, though, to explain why the 1548 Å line would be weaker than the 1550 Å line. A broad P Cygni absorption component of the 1550 line may be required, with ~ -400 km s^{-1} as suggested by Keyes and Plavec for AG Peg, making the RX Pup C IV profiles very complicated indeed.

In Figure 1 we show the SWP (*top*) and LWR (*bottom*) low dispersion spectra of RX Puppis. In Figures 2, 3, 4 and 5 we show the N IV], C IV, O III], He II, Si III] high-resolution profiles discussed above.

These figures show how important it is to obtain high-dispersion spectra of symbiotic stars, whenever feasible. On the basis of the low-dispersion spectra alone, one may be tempted to conclude that RX Pup appears similar to RW Hya (Kafatos, Michalitsianos, and Hobbs 1980). A comparison, though, of high-dispersion spectra of these two stars reveal fundamental differences: Strong dynamic activity is suggested in the spectra of RX Pup. On the other hand, strong emission in N V, O I, Si IV, O IV, He II, O III], N III], Si III], C III], C II], Mg II, and O III was seen in RW Hya with no indication of split profiles or absorption features (Kafatos, Michalitsianos, and Hobbs 1980). In another respect, the differences between these stars were noted by Feast, Robertson, and Catchpole (1977): RW Hya is a symbiotic star without dust, whereas RX Pup (along with RR Tel, a slow nova) is a member of a symbiotic system that exhibits thermal dust emission (cf. Swings and Allen 1972). Moreover, such objects as RR Tel, RX Pup, and PKS 280−2.1 (Feast, Robertson, and Catchpole 1977) have been compared to slow novae, but a clear distinction between novae and peculiar emission line stars has not been established.

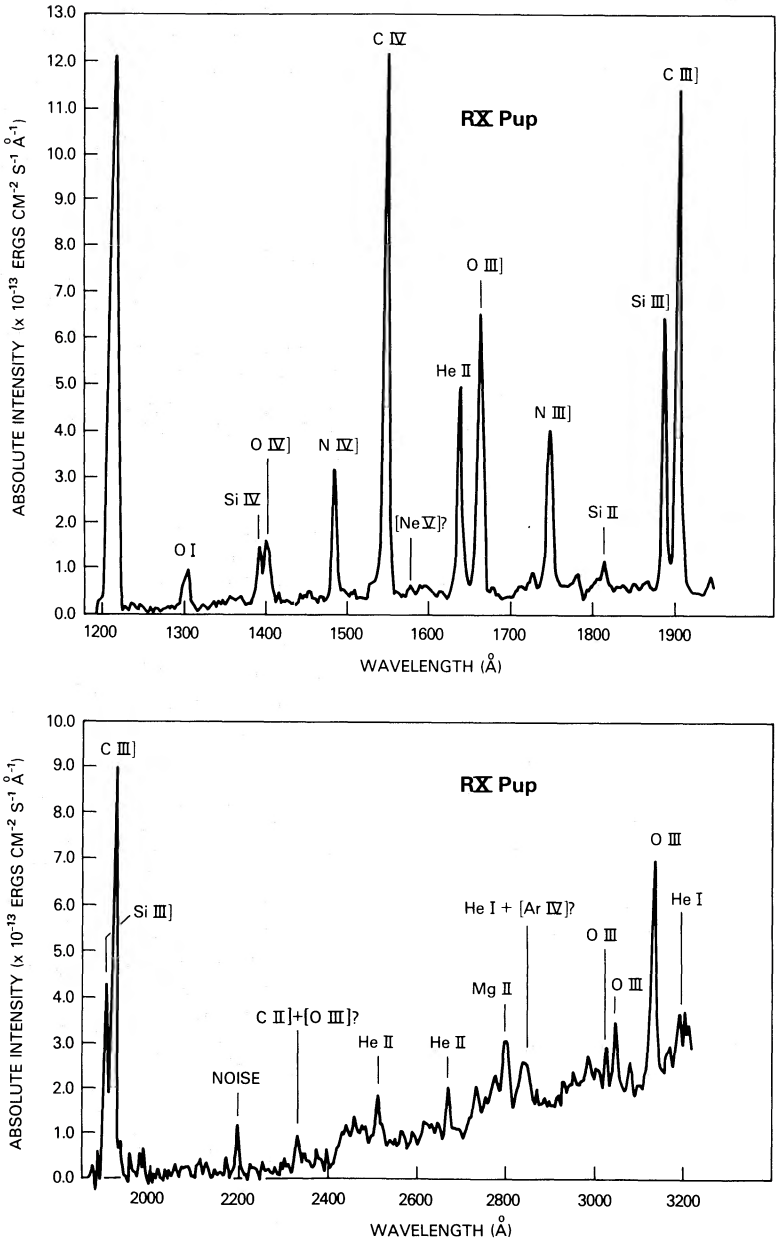

FIG. 1.—SWP (top) and LWR (bottom) low-dispersion spectra of RX Puppis

In Figure 1 a continuum is evident, weak but slowly rising toward longer wavelengths in SWP and quite strong and rapidly rising in LWR. It is not possible to obtain an exact value of the extinction from the 2200 Å dip, although it is clear that absorption is not negligible (but still $E_{B-V} \lesssim 1$). Klutz, Simonetto, and Swings (1978) obtained a value of ~ 1 kpc for the distance to this object. Using a galactic absorption law (Kafatos, Michalitsianos, and Hobbs 1980), we find $E_{B-V} \approx 0.7$. Klutz, Simonetto, and Swings (1978) favor E_{B-V} in the range 0.7–1.0. Feast, Robertson, and Catchpole (1977), on the other hand, obtained $E_{B-V} \sim 0.3$. We also estimated E_{B-V} from the theoretical ratios of the He II lines (cf. Seaton 1978) and found that $E_{B-V} \geq 0.7$. This method is, though, suspect because it is not clear how the ratios would vary at the high densities prevalent in the RX Pup nebula. Henceforth, in our analysis, we will assume values of $E_{B-V} = 0.3$ or 0.7.

The simplest approach one can take to explain the continuum is to attribute it to a photospheric continuum from a hot companion. This has been a useful approach for a number of binary stars (Parsons 1981). In symbiotic stars, though, this approach has been generally unsatisfactory (Michalitsianos *et al.* 1982; Kafatos 1981). We find that the UV continuum mimics that of an early

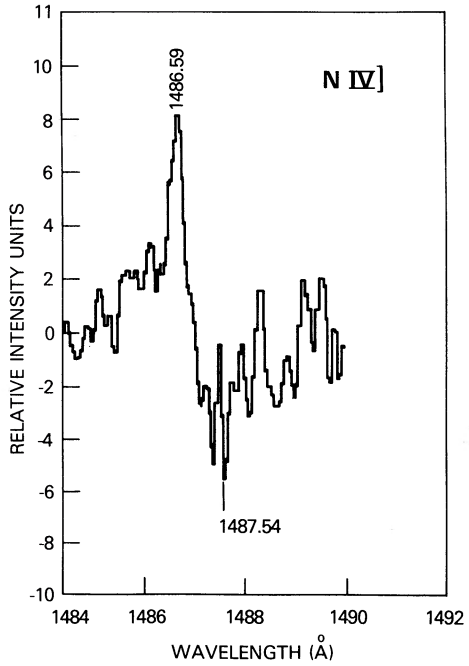

FIG. 2.—N IV] profile (high-dispersion)

F to an early A type, depending on the value of E_{B-V} (A8 II, $M_V \sim -1.9$ for $E_{B-V} = 0.3$; and A0 II, $M_V \sim -3.16$ for $E_{B-V} = 0.7$). If the continuum is from a star it cannot be earlier than A0 (because it would have been brighter than 9th magnitude at the time of our observation). From this we deduce that there is no evidence for a B star in RX Pup (cf. Klutz, Simonetto, and Swings 1978.)

We suspect that alternative continuum emission mechanisms may be required: nebular bound-free and free-free continuum (see § II*b*) and/or continuum from a boundary layer and accretion disk (see § III). Observations over different times would help us in discerning the nature of the continuum (if it is constant, it would probably be from star; if it varies, it would be from an accretion disk or a gas stream).

b) *Nebular Parameters*

The UV spectrum of RX Pup is dominated by allowed and semiforbidden lines. In the previous section we saw that the high-resolution profiles indicate a number of distinct regions in velocity space. In order to obtain information about the densities and temperatures prevalent in the line emitting regions, we make the simplifying assumption that uniform densities and temperatures prevail in these regions; the densities and temperatures we thus obtain should be taken as rough values. This simplifying assumption turns out to be fairly valid.

The semiforbidden lines are sensitive to the density. We obtain lower limits on the electron density, $n_e \gtrsim 10^6$ cm^{-3}, from the absence of the C III] 1906.7 Å line and the N IV] 1483.2 Å line (Loulergue and Nussbaumer 1976). Moreover, the presence of the N IV] 1486.5 Å line implies $n_e \lesssim 10^{11}$ cm^{-3}, and the presence of the C III] 1908.7 Å line implies $n_e \lesssim 2 \times 10^{10}$ cm^{-3} (Osterbrock 1970).

The strength of the C III] 1908.7 Å line relative to the $\lambda\lambda$1174.93–1176.38 C III multiplet which was possibly detected gives estimates of the density as well as upper limits of the electron temperature T_e (cf. Loulergue and Nussbaumer 1974, 1976; Nussbaumer and Schild 1979). We find that $T_e \lesssim 30{,}000$ K and $10^9 \lesssim n_e \lesssim 10^{10}$ cm^{-3}. Similarly, the N III] multiplet can be used to obtain estimates of n_e (cf. Altamore *et al.* 1981; Nussbaumer and Storey 1979). We find that $n_e \sim 2 \times 10^{10}$ cm^{-3}, although a density gradient may be necessary. The situation with the O IV] multiplet is less clear due to the weakness of the lines: higher densities ($n_e \sim 10^{11}$ cm^{-3}) may be required, but deeper exposures are needed (cf. Flower and Nussbaumer 1975).

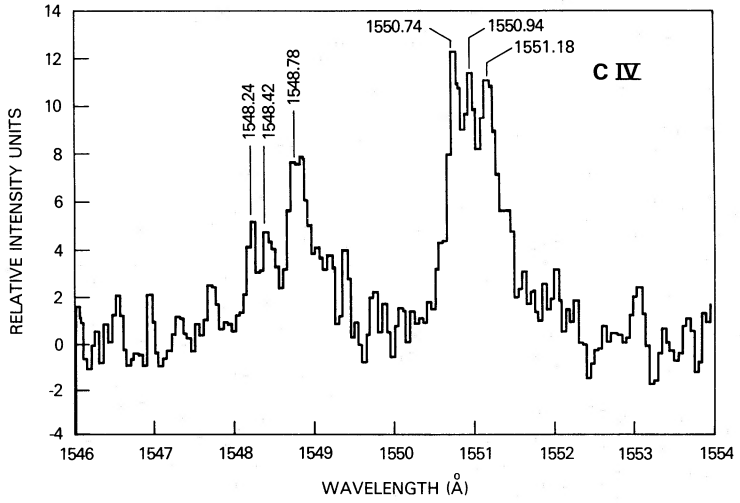

FIG. 3.—C IV profiles (high-dispersion)

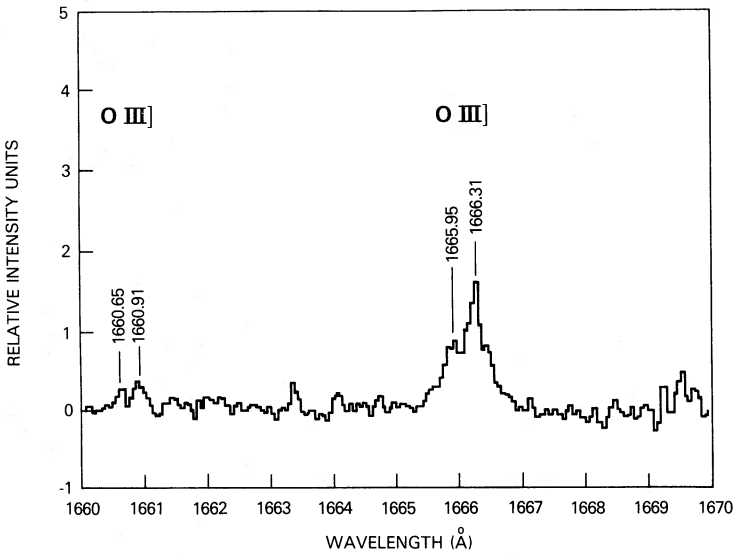

FIG. 4.—O III] profiles (high-dispersion)

The weakness or total absence of forbidden-line emission also argues for high densities. The presence of the [Ne V], [Ne III] lines is questionable. From Kafatos and Lynch (1980) we find that the [Ne V] 1575.2 Å, [Ne IV] 1601.5 Å, and [Ne III] 1814.8 Å lines get collisionally depopulated near $n_e \sim 10^8$ cm^{-3}. Since no [Ne IV] feature was seen, if the [Ne III], [Ne V] lines are present this would imply $n_e \gtrsim 10^{10}$ cm^{-3}. The only forbidden lines that may exist in the low-resolution LWR spectrum are λ2321.1 [O III] (although blended with C II] λ2325–λ2328) and [Ar IV] λ2853.6 (again blended with He I λ2829.1). It may indeed be the case that no forbidden lines are present in the *IUE* spectra. The absence of the [O II] λ2471 implies $n_e \gtrsim 10^9$ cm^{-3} for $T_e \sim 15{,}000$ K (Kafatos and Lynch 1980). Klutz and Swings (1981) obtained recently coude spectra of RX Pup. They find that the ratio of the [O III] 4363 Å to the $N_1 + N_2$ lines is high, indicating high densities.

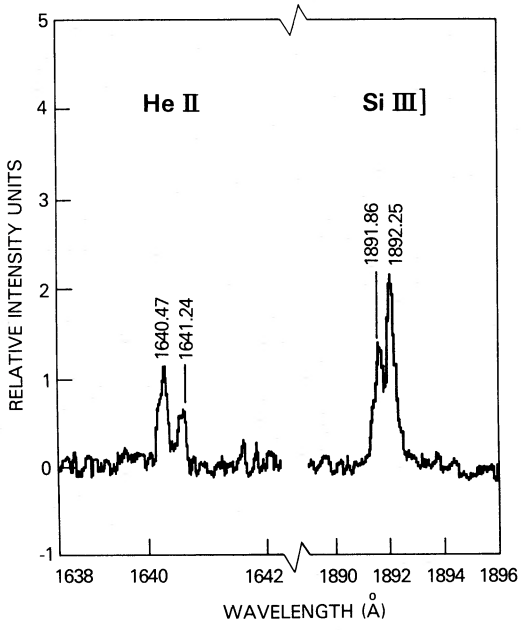

FIG. 5.—He II and Si III] profiles (high-dispersion)

From the previous discussion it follows that the various semiforbidden and forbidden intensities imply densities in the range from 10^9 to a few times 10^{10} cm^{-3}, with upper limits not more than 10^{11} cm^{-3}. All lines could arise from a single density region ($n_e \sim 10^{10}$ cm^{-3}), although this statement depends obviously on whether a single value of T_e applies to all lines.

The absolute intensities of the UV lines can be used to estimate the relative ionic abundances in the line emitting region. For densities up to a few times 10^9 or a few times 10^{10} cm^{-3} the semiforbidden line strengths are proportional to $n_e^2 L\Omega$, where L is the path length through the emitting region (Kafatos, Michalitsianos, and Hobbs 1980) and Ω the solid angle of the region. This expression reduces to $n_e^2 L^3$ for a spherical region, where L is the size. If the region, however, is in the form of streams, rings, or a disk, we have to take into account the geometrical effects of observation. In general, we can always write it as $n_e^2 L^3 f_g$, where $f_g \leq 1$ is a factor depending on the geometry of the region relative to the line of sight and the equality applies in the spherical case. In the general case, L is understood to be the largest characteristic size of the region (e.g., the diameter of the disk, etc.). Since the line intensities are proportional to $n_e^2 L^3 f_g$, if we set $f_g = 1$ and we substitute a value for n_e ($\sim 10^9$–10^{10} cm^{-3}), the resultant value for L is a *lower limit*.

In Table 2 we show the relative ionic abundances for the following adopted parameters: $E_{B-V} = 0.3$, $T_e = 15{,}000$ K, distance $d = 1000$ pc (Klutz, Simonetto, and Swings 1978). The inequalities apply because some N II,

TABLE 2

IONIC ABUNDANCES
($E_{B-V} = 0.3$, $d = 1000$ pc, $T_e = 15{,}000$ K)

Ion	Relative Ionic Abundance
He I	0.17
He II	0.66
He III	0.17
C II	0.16
C III	0.46
C IV	0.38
N II	...[a]
N III	<0.71
N IV	<0.29
O II	...[a] (<0.46)[b]
O III	<0.87 (>0.47)[b]
O IV	<0.13 (>0.07)[b]
Si II	<0.07
Si III	<0.63
Si IV	<0.30
Si V	...[a]
Mg II	0.005[c]

[a] Some N II, O II, and Si V should be present.
[b] From upper limit to the [O II] line flux.
[c] Applicable if Mg II emission comes from line emission region rather than being chromospheric.

O II, and Si V should be present, although the exact amounts are unknown due to the lack of observable lines. The Mg II emission may, on the other hand, arise from the chromosphere of the red giant, although single Miras observed before (Kafatos, Michalitsianos, and Hobbs 1980) show much weaker Mg II emission. In Table 3A we show the lower limit of the larger dimension of the region L, for values of electron density $n_e = 10^9$, 10^{10} cm^{-3}. The ionic abundances depend very weakly on the value of the extinction assumed. We computed a different model for $E_{B-V} = 0.7$ with substantially the same results, except for He I and He II. The values of L change by a factor of ~ 3 when $E_{B-V} = 0.7$ is assumed, and are shown in Table 3B.

The chemical abundances for the nebular model of Table 2 are cosmic for nitrogen and oxygen. Carbon is, however, depleted by a factor of ~ 7 and silicon by ~ 4 with respect to cosmic abundances. Similar situation prevails in other symbiotic stars—e.g., R Aqr (Michalitsianos, Kafatos, and Hobbs 1980) and RW Hya (Kafatos, Michalitsianos, and Hobbs 1980).

TABLE 3

LARGER DIMENSION OF REGION

n_e(cm^{-3})	L(cm)
A. $E_{B-V} = 0.3$	
10^9	$\geq 3.7 \times 10^{13}$[a]
10^{10}	$\geq 8.1 \times 10^{12}$[a]
B. $E_{B-V} = 0.7$	
10^9	$\geq 9.7 \times 10^{13}$[a]
10^{10}	$\geq 2.1 \times 10^{13}$[a]

[a] Equality applies if region is spherical ($f_g = 1$; see text).

The nebular parameters depend strongly on the assumed value of T_e. Since forbidden line emission is weak or totally absent, we have no independent way to determine T_e. We already saw that a probable upper limit for T_e is $\sim 30{,}000$ K. Moreover, we can rule out chromospheric transition region temperatures of the order of or greater than 100,000 K. At $T_e \sim 10^5$ collisional ionization would be the dominant mechanism and ionic abundances would be different than the values listed in Table 2 (cf. Kafatos 1973). We believe that T_e is in the probable range $\sim 10^4$ to 2×10^4 K expected for a nebula that is photoionized, with an upper limit of $\sim 30{,}000$ K. Without an independent way to determine the product $n_e^2 L^3 f_g$ or the chemical abundances, the value $T_e = 15{,}000$ K adopted in Table 2 is only suggestive. Even with the uncertainties involved, however we disagree with the contention of Altamore *et al.* (1981) that a transition region around the cool star in Z And is required for the line emission. A similar analysis can be applied to that symbiotic star too, and we find that temperatures $\sim 10^5$ K are ruled out as in RX Pup for similar reasons. We agree, however, with Nussbaumer and Schild (1981), who find that photoionization dominates in V1016 Cyg as well.

We also note that for $E_{B-V} = 0.3$ free-free and bound-free continuum would contribute about a fifth of the observed continuum in the LWR region of the spectrum and slightly less than this value in the SWP. For $E_{B-V} = 0.7$, $T_e = 15{,}000$ K the theoretical continuum would be roughly half of the observed continuum in the LWR region. It suffices to say here that bound-free and free-free continua make a substantial contribution to the observed continuum, particularly for the higher values of E_{B-V} considered.

The Bowen resonance-fluorescence lines of O III can be used to estimate the number of photons below 228 Å (the He II Lyman continuum photons). The 3132.86 Å O III line contributes ~ 0.31 of the total fluorescence line flux (Osterbrock 1974). Moreover, the overall fraction of He II Lyα photons converted into Bowen resonance-fluorescence photons is ~ 0.5 (Osterbrock 1974). Since the nebula is thick in the He II Lyman lines, recombinations of He III to all levels $n \geq 2$ yield He II Lyα photons (Seaton 1960). The observed 3132.86 Å flux, therefore, implies that $N(h\nu \geq 54.4 \text{ eV}) \sim 4.6 \times 10^{44}$ s^{-1} for $E_{B-V} = 0.3$ and $N(h\nu \geq 54.4 \text{ eV}) \sim 3.1 \times 10^{45}$ s^{-1} for $E_{B-V} = 0.7$.

III. DISCUSSION AND CONCLUSIONS

We saw in § II*b* that photionization seems to dominate in the line emitting region of RX Pup. The question remains: What is the source of the UV photons? In the present section we attribute the photoionization either to (*a*) a hot companion or (*b*) to an accretion disk/boundary layer. A combination of these two cases (*a*) and (*b*) is, of course, also possible.

a) Hot Companion

If we attribute the observed continuum to an early F or an early A star (§ II*a*), we find that such a star does not emit enough ionizing photons to produce the line emitting region: We need a considerably hotter star in this case.

We have obtained an approximate distribution of the ionizing continuum flux F_ν below 912 Å by using the relative ionic abundances of Table 2 and evaluating the product $F_\nu a_\nu$ at the threshold of each ion, where a_ν is the photoionization cross section (cf. Osterbrock 1974). In this procedure, we have assumed that the size of the ionization region for each ion is constant, an obvious simplifying assumption. We have compared this approximate flux F_ν with the LTE models of Hummer and Mihalas (1970). We find that the effective temperature of the secondary star is in the approximate range 4×10^4 K $\lesssim T_{\rm eff} \lesssim 10^5$ K: If $T_{\rm eff}$ were lower than the lower limit (if T were, say, equal to 30,000 K), the ionizing flux—whether blackbody or from the model atmosphere—would be too small below ~760 Å to explain the ionization beyond Si II; if, on the other hand, $T_{\rm eff}$ were above the upper limit, then there would be too much flux below 160 Å and the N V, O V lines should be present and strong in the SWP spectrum of RX Pup. We also find that a non-LTE pure hydrogen model atmosphere at $T_{\rm eff} = 55{,}000$ K (Holberg *et al.* 1980) provides a reasonable fit (within a factor of ~2) to our estimated values of F_ν, the greater discrepancies occurring at the C III, He I, Si II, and Mg II ionization limits. In what follows, for both the photoionizing flux from a hot companion and/or the photoionizing flux from a boundary layer-accretion disk we will assume that the temperatures are in the range 40,000 K–100,000 K.

From the Strömgren relation we find that the number of ionizing photons, N_i, is $\sim 4.9 \times 10^{45}$ s^{-1} for $E_{B-V} = 0.3$ and $\sim 8.6 \times 10^{46}$ s^{-1} for $E_{B-V} = 0.7$. The results of Hummer and Mihalas (1970) show that the overall number of ionizing (beyond the Lyman limit) photons in their models is not greatly different from the estimated number of photons that arise from a blackbody. We therefore use the blackbody formula and find the values of R_*, the radius of the secondary, required to produce enough ionizing photons N_i values that are shown in Table 4A for the two values of $E_{B-V} = 0.3$, 0.7 and the two limits of the effective stellar temperature, $T_{\rm eff} = 40{,}000$ K and 100,000 K. We see that if a hot companion is responsible for the photoionizing radiation, such a star would be located in the central stars of planetary nebulae region and near the location of the hot companion in RW Hya (Kafatos, Michalitsianos, and Hobbs 1980).

The estimated number of photons with energy ≥ 54.4 eV (§ II*b*) can be compared with the theoretical values

TABLE 4

A. Photoionization from a Hot Companion

E_{B-V}	$R_*/R_\odot$	$L_*/L_\odot$
$T_{\rm eff} = 40{,}000$ K		
0.3	0.21	100
0.7	0.88	1.7×10^3
$T_{\rm eff} = 100{,}000$ K		
0.3	0.027	65
0.7	0.11	1.1×10^3

B. Photoionization from an Accretion Disk/Boundary Layer around a Secondary

Parameter	Case A[a]	Case B[b]	Case C[c]	Case D[d]
R_9	117	490	15.4	63.7
M_{-8}	6.9×10^2	5.1×10^4	60	4.4×10^3
L_d	62.1	1.1×10^3	42	7.2×10^2
$L_T/L_{\rm Edd}$	5.2×10^{-3}	9.2×10^{-2}	3.5×10^{-3}	6.1×10^{-2}
β	1.3×10^{-6}	3×10^{-7}	9.6×10^{-6}	2.3×10^{-6}
i	60°	73°	57°	72°

[a] Case A: $E_{B-V} = 0.3$, $T_{\rm bl} = 40{,}000$ K, $N_i = 4.9 \times 10^{45}$ s^{-1}, $L_{\rm obs}^{\rm UV} = 30\ L_\odot$.
[b] Case B: $E_{B-V} = 0.7$, $T_{\rm bl} = 40{,}000$ K, $N_i = 8.6 \times 10^{46}$ s^{-1}, $L_{\rm obs}^{\rm UV} = 300\ L_\odot$.
[c] Case C: $E_{B-V} = 0.3$, $T_{\rm bl} = 100{,}000$ K, $N_i = 4.9 \times 10^{45}$ s^{-1}, $L_{\rm obs}^{\rm UV} = 30\ L_\odot$.
[d] Case D: $E_{B-V} = 0.7$, $T_{\rm bl} = 100{,}000$ K, $N_i = 8.6 \times 10^{46}$ s^{-1}, $L_{\rm obs}^{\rm UV} = 300\ L_\odot$.

Note.—$T_{\rm bl}$, boundary layer temperature (K). N_i, number of ionizing ($h\nu \gtrsim 13.6$ eV) photons (s^{-1}). $L_{\rm obs}^{\rm UV}$, portion of disk and boundary layer luminosity emitted in the *IUE* spectral range, determined from the observed flux and the distance (in $L_\odot$). R_9, radius of secondary (in 10^9 cm). $\dot{M}_{-8}$, accretion rate onto secondary (in $10^{-8}\ M_\odot$ yr^{-1}). L_d, L_T, $L_{\rm Edd}$, disk, total, and Eddington luminosities ($L_\odot$). β, efficiency of accretion. i, angle between the normal to the orbital plane and the line of sight.

of the same quantity from Hummer and Mihalas (1970). We find that models with 75,000 K $\lesssim T_{\rm eff} \lesssim$ 90,000 K and $4.5 \lesssim \log g \lesssim 5.5$ provide reasonable agreement. The effective stellar temperature can be as high as 10^5 K ($\log g = 6$ model of Hummer and Mihalas 1970) but certainly not above this value or lower than $\sim$70,000 K.

We conclude that effective temperature values above halfway in the range 40,000 K–100,000 K are probably the best estimates (say, $T_{\rm eff} \gtrsim$ 75,000 K but still $T_{\rm eff} \lesssim 10^5$ K).

b) Accretion Disk around a Secondary

The photoionizing photons may alternatively arise from an accretion disk and its inner boundary layer region. As we noted, the velocity structure of the line profiles is suggestive of rings of material around and/or streamers onto a secondary. We note that although our model of an accretion disk may not explain the UV spectral properties of RX Pup at all times, it nevertheless presents an interesting theoretical limit: if accretion fully develops, the parameters required are given below.

We use the relations derived by Kafatos (1981) to estimate the various accretion parameters (see also Bath *et al.* 1974; Tylenda 1977; Lynden-Bell and Pringle 1974). These parameters are shown in Table 4B and are the following: R_9 is the radius of the secondary in 10^9 cm; $\dot{M}_{-8}$ is the accretion rate onto the secondary in 10^{-8} $M_\odot$ yr^{-1} (we have assumed the mass of the secondary to be equal to 1 $M_\odot$); L_d is the disk luminosity in solar units; L_T, $L_{\rm Edd}$ are the total (boundary layer plus disk) and Eddington luminosities, respectively; β is the efficiency of accretion defined by $\beta = L_T/\dot{M}c^2$; and i is the angle between the normal to the orbital plane and the line of sight.

As in § III*a* we have assumed that the maximum temperature in the inner region of the disk, $T_{\rm bl}$, in the range 40,000 K–100,000 K. We compute the accretion parameters for two values of $E_{B-V} = 0.3, 0.7$. The number of ionizing photons emitted by the boundary layer is set equal to 4.9×10^{45} s^{-1} for $E_{B-V} = 0.3$ and 8.6×10^{46} s^{-1} for $E_{B-V} = 0.7$ (the values shown in Table 4B are for the case of the ionized region being ionization bounded) as obtained by the analysis of § II. Finally, the observed UV luminosity in the *IUE* range (i.e., for $1200 \leq \lambda \leq 3200$ Å), $L_{\rm obs}^{\rm UV}$, can be obtained if we set the distance equal to 1000 pc; it is equal to 30 $L_\odot$ for $E_{B-V} = 0.3$, 300 $L_\odot$ for $E_{B-V} = 0.7$. In Table 4B we distinguish four cases: cases A and B for $T_{\rm bl} = 40{,}000$ K, cases C and D for $T_{\rm bl} = 100{,}000$ K, cases A and C for $E_{B-V} = 0.3$, cases B and D for $E_{B-V} = 0.7$. We first note that since $T_{\rm bl}/T_d\,(r = 2.25\,R_*) \sim 5.81$ (Tylenda 1977), the SWP and LWR flux would be due primarily to the disk if $T_{\rm bl} \lesssim$ 80,000 K. For $T_{\rm bl} = 40{,}000$ K the disk would mimick an F2 star whereas for $T_{\rm bl} = 100{,}000$ K it would mimic a B4 star. The observed *IUE* continuum flux could, therefore, arise from an accretion disk. We note, however, that since the densities in the line emitting region are in the range $\sim 10^9$–10^{10} cm^{-3}, the semi-forbidden lines cannot arise in a disk where the expected densities would be $n_e \gtrsim 10^{18}$ cm^{-3} in the inner region.

The number of photons with $h\nu \gtrsim 54.4$ eV obtained by the O III fluorescence line analysis can be used to estimate the temperature of the boundary layer. We have $N(h\nu \gtrsim 54.4\ {\rm eV})/N(h\nu \gtrsim 13.6\ {\rm eV}) \sim 0.095,\ 0.037$ for $E_{B-V} = 0.3$ and 0.7, respectively. Using the blackbody formulae, we find that $T_{\rm bl} \sim 1.1 \times 10^5$ K and 9×10^4 K, respectively. We therefore see that the boundary layer temperature is again closer to the upper limit of the estimated range $\sim 10^5$ K.

We see from Table 4B that the derived radius of the companion star may indeed indicate that a main sequence star (cases A, B, and D), rather than a hot subdwarf, is present. Accretion rates for cases A, B, and D are also more indicative of accretion onto a main sequence star (Michalitsianos *et al.* 1981). A similar situation has been shown to exist in CI Cygni (Stencel *et al.* 1982; Bath and Pringle 1980). The small values of $L_T/L_{\rm Edd}$ indicate, though, that the supercritical accretion model of Bath (1977) does not apply, at least at present.

Whether photoionization from a hot subdwarf or photoionization from a boundary layer/accretion disk around a cooler main sequence star is required is unclear at present. Undoubtedly, symbiotic stars where a hot secondary is present exist (e.g., R. W. Hya; see Kafatos, Michalitsianos, and Hobbs 1980); as well as symbiotic stars where a main sequence secondary—with an accretion disk—exists (e.g., CI Cyg; see Stencel *et al.* 1981).

A possible test may be provided by future observations. Using the effective temperature of the Mira of 2400 K (Barton, Phillips, and Allen 1979) and the theoretical relations for Miras of Willson (1980), we find the expected period of the Mira in RX Pup to be $\gtrsim$700 days (close to the value of 580$^{\rm d}$ reported by Whitelock 1981), its radius $\sim$600 $R_\odot$, its mass $\sim$2–3 $M_\odot$, and its luminosity $\sim 10^4$ $L_\odot$. The expected mass loss rate would be $\sim 3 \times 10^{-7}$ $M_\odot$ yr^{-1}, less than all the values of the accretion rate of Table 4B: Mass loss, therefore, is enhanced, very likely because of binarity. If the Mira were filling its Roche lobe, the system would have a period $\lesssim$8 yr. Observations in the next few years of this very interesting object would be very important to see whether a short orbital period exists, i.e., a Roche overflow situation. In that case a main sequence secondary would be indicated (otherwise the disk luminosity would be excessive). Monitoring RX Pup is important, in any case, because it appears that it is returning to a symbiotic phase (Klutz and Swings 1981).

One thing is clear: The peculiar line profiles in RX Pup would be hard to interpret in terms of a single star only. If we set the stream velocity ($\sim$100–200 km s^{-1}) equal to the escape velocity at distance r from the star, we find that $r \gtrsim 10^{12}$ cm, comparable to the radius of the line emitting region. The symmetric profiles argue for the presence of rings.

We thank R. Viotti and particularly J. P. Swings for useful comments and suggestions.

REFERENCES

Allen, D. A. 1979, in *IAU Colloquium 46, Changing Trends in Variable Star Research*, ed. F. M. Bateson, J. Smak, and I. H. Urch (preprint).
———. 1980, *M.N.R.A.S.*, **190**, 75.
Altmore, A., Baratta, G. B., Cassatela, A., Friedjung, M., Giangrande, A., Ricciardi, O., and Viotti, R. 1981, *Ap. J.*, **245**, 630.
Barton, J. R., Phillips, B. A., and Allen, D. A. 1979, *M.N.R.A.S.*, **187**, 813.
Bath, G. T. 1977, *M.N.R.A.S.*, **178**, 203.
Bath, G. T., Evans, W. D., Papaloizou, J., and Pringle, J. E. 1974, *M.N.R.A.S.*, **169**, 447.
Bath, G. T., and Pringle, J. E. 1980, *M.N.R.A.S.*, **194**, 967.
Boggess, A., *et al.* 1978, *Nature*, **278**, 372.
Bruhweiler, F. C., and Kondo, Y. 1981, *Ap. J.* (*Letters*), **248**, L123.
Bruhweiler, F. C., Kondo, Y., and McCluskey, G. E. 1980, *Ap. J.*, **237**, 19.
Fahey, R. P., and Klingesmith, D. A. 1979, *IUE FORTH Spectral Analysis User's Guide* (NASA Tech. Note X-685-79-29).
Feast, M. W., Robertson, B. S. C., and Catchpole, R. M. 1977, *M.N.R.A.S.*, **179**, 499.
Flower, D. R., and Nussbaumer, H. 1975, *Astr. Ap.*, **45**, 145.
Holberg, J. B., Sandel, B. R., Forrester, W. T., Broadfoot, A. Lyle, Shipman, H. L., and Barry, D. C. 1980, *Ap. J.* (*Letters*), **242**, L119.
Hummer, D. G., and Mihalas, D. 1970, *M.N.R.A.S.*, **147**, 339.
Kafatos, M. 1973, *Ap. J.*, **182**, 433.
———. 1981, in *IAU Colloquium 70*, ed. R. Viotti, in press.
Kafatos, M., and Lynch, J. P. 1980, *Ap. J. Suppl.*, **42**, 611.
Kafatos, M. Michalitsianos, A. G., and Hobbs, R. W. 1980, *Ap. J.*, **240**, 114.
Kelly, R. L. 1979, *Atomic Emission Lines in the Near Ultraviolet*, TM 80268.
Kelly, R. L., and Palumbo, L. J. 1973, *Atomic and Ionic Emission Lines Below 2000 Angstroms*, NRL Report 7599.
Keyes, C. D., and Plavec, M. J. 1980, in *IAU Colloquium 88, Close Binary Stars: Observations and Interpretation*, ed. M. J. Plavec, R. K. Popper, and R. K. Ulrich (Dordrecht: Reidel), p. 535.
Klutz, M., Simonetto, O., and Swings, J. P. 1978, *Astr. Ap.*, **66**, 283.
Klutz, M., and Swings, J. P. 1981, *Astr. Ap.*, **96**, 406.
Loulergue, M., and Nussbaumer, H. 1974, *Astr. Ap.*, **34**, 63.
———. 1976, *Astr. Ap.*, **51**, 163.
Lynden-Bell, D., and Pringle, J. E. 1974, *M.N.R.A.S.*, **168**, 603.
Michalitsianos, A. G., Kafatos, M., Feibelman, W. A., and Hobbs, R. W. 1982, *Ap. J.*, **253**, 735.
Michalitsianos, A. G., Kafatos, M., and Hobbs, R. W. 1980, *Ap. J.*, **237**, 506.
Nussbaumer, H., and Schild, H. 1979, *Astr. Ap.*, **75**, L17.
———. 1981, *Astr. Ap.*, in press.
Nussbaumer, H., and Storey, P. J. 1979, *Astr. Ap.*, **71**, L5.
Osterbrock, D. E. 1970, *Ap. J.*, **160**, 25.
———. 1974, *Astrophysics of Gaseous Nubulae* (San Francisco: Freeman).
Parsons, S. B. 1981, *Ap. J.*, **247**, 560.
Sanduleak, N., and Stephenson, C. B. 1973, *Ap. J.*, **185**, 899.
Seaton, M. J. 1960, *Rep. Progr. Phys.*, **23**, 313.
———. 1978, *M.N.R.A.S.*, **185**, 5p.
Seitter, W. C. 1971, in *IAU Colloquium 15, New Directions and New Frontiers in Variable Star Research* (Bamberg).
Stencel, R. E., Michalitsianos, A. G., Kafatos, M., and Boyarchuk, A. A. 1982, *Ap. J.* (*Letters*), **253**, in press.
Swings, P. 1970, in *Spectroscopic Astrophysics*, ed. G. H. Herbig (Los Angeles: University of California Press).
Swings, J. P., and Allen, D. A. 1972, *Pub. A.S.P.*, **84**, 523.
Swings, J. P., and Klutz, M. 1976, *Astr. Ap.*, **46**, 303.
Swings, J. P., and Struve, O. 1941, *Ap. J.*, **94**, 291.
Tylenda, R. 1977, *Acta Astr.*, **27**, 235.
Whitelock, P. 1981, in *IAU Colloquium 70*, ed. R. Viotti, in press.
Wiese, W. L., Smith, M. W., and Glennon, B. M. 1966, *Atomic Transition Probabilities*, Vol. **1** (NSRDS–NBS4).
Willson, L. A. 1980, in *Physical Processes in Red Giants*, ed. A. Renzini and I. Iben (Erice).

W. A. Feibelman and A. G. Michalitsianos: Code 685.1, Laboratory for Astronomy and Solar Physics, NASA Goddard Space Flight Center, Greenbelt, MD 20771

M. Kafatos: Department of Physics, George Mason University, Fairfax, VA 22030